Detecting newly-formed Labrador Sea Water from space

R. Gelderloos,[1] C. A. Katsman,[1] K. Våge,[2]

R. Gelderloos, Global Climate Division, Royal Netherlands Meteorological Institude, P.O. Box 201, 3730 AE De Bilt, Netherlands (renske.gelderloos@knmi.nl).

C. A. Katsman, Global Climate Division, Royal Netherlands Meteorological Institude, P.O. Box 201, 3730 AE De Bilt, Netherlands.

K. Våge, Geophysical Institute, University of Bergen, Allegaten 70, 5007 Bergen, Norway

[1]Global Climate Division, Royal Netherlands Meteorological Institute, De Bilt, Netherlands.

[2]Geophysical Institute, University of Bergen, Bergen, Norway.

Abstract. In situ monitoring of deep water formation in the Labrador Sea is severely hampered by the harsh winter conditions in this area. Furthermore, the ongoing monitoring programs do not cover the entire Labrador Sea and are often summer observations. The network of satellite altimeters does not suffer from these limitations and could therefore give valuable additional information. Altimeters can in theory detect deep water formation, because the water column becomes denser during convection and therefore the sea surface becomes lower. This signal is small compared to variability in sea surface height induced by other sources, and due to substantial eddy-induced variability a clear one-to-one relation between the local mixed layer depth and the local sea surface height variations at a given location and time is not found in the Labrador Sea. However, if properly averaged in time and space all three winters with deep convection exceeding 1500 m depth in the 1994-2009 period clearly stand out. Furthermore, for 12 out of the other 13 winters the distinction between convection deeper or shallower than 1000 m could be made. This required a more thorough analysis of the data than only averaging, but careful inspection of the SSH fields distinguishes convective activity from (primarily wind-driven) gyre-scale variations.

1. Introduction

The Labrador Sea area is known for its very harsh winter conditions. If the winds over this part of the ocean are sufficiently strong and cold, and the oceanic conditions are favorable, they can cause deep convection down to more than two kilometers depth [*Marshall and Schott*, 1999; *Yashayaev*, 2007]. The product of deep convection, known as Labrador Sea Water (LSW), subsequently spreads into the North Atlantic region and beyond [*Talley and McCartney*, 1982; *Bower et al.*, 2009]. It thus partly sets the density structure at intermediate depth, and thereby plays an important role in setting the strength and shape of the Atlantic meridional overturning circulation [AMOC; *Kuhlbrodt et al.*, 2007]. This is supported by several model simulations, which have shown a strong correlation between variability in LSW formation and the strength of the AMOC on interannual to decadal timescales [*Eden and Willebrand*, 2001; *Biastoch et al.*, 2008].

LSW formation displays a large interannual variability. Over the period of the observational record, the mixed layer depth (MLD) showed a range of about 200 m to 2400 m [*Yashayaev*, 2007], an order of magnitude variation. Given the important role LSW formation is considered to play in the variability of the AMOC strength, it is very important to properly monitor this substantial variability. In situ monitoring is, however, severely hampered by the harsh winter conditions on site.

Over the past decades several observational programs have been undertaken in an effort to monitor LSW formation (see Figure 1 for the locations of the different long-term observational programs). The first data set showing interannual variability of LSW formation was collected at the US Coast Guard's Ocean Weather Station (OWS) Bravo, which was located in the southwestern part of the central Labrador Sea. Between 1964 and 1974 regular oceanographic measurements were taken, which provided a time series that includes both winters with intense deep convection as well as a multiple-year shutdown [*Lazier*, 1980]. From 1990 onwards, a hydrographic section known as AR7W has been occupied annually by the Canadian Bedford Institute of Oceanography [*Yashayaev*, 2007] as part of the World Ocean Circulation Experiment (WOCE). For practical reasons, the hydrographic section is usually taken in spring, summer or autumn and therefore only shows the water mass produced by wintertime deep convection. A few wintertime hydrographic observations are available as well. In particular, two winter cruises (in 1997 and 1998) were undertaken as part of the Labrador Sea Deep Convection Experiment [*LabSeaGroup*, 1998], one of which measured during active convection [*Pickart et al.*, 2002]. Earlier wintertime hydrographic programs were undertaken in 1962, 1966, 1976 and 1978 [*Lilly et al.*, 1999]. As wintertime measurements are difficult to obtain in this region, a mooring was placed on the AR7W line close to the original location of OWS Bravo. This mooring has provided an almost continuous full-depth record of convective activity at that particular location from 1996 to 2003 [*Avsic et al.*, 2006].

A different type of observational tool is the network of autonomous profiling floats [*Roemmich et al.*, 2009; *Roemmich, D. and the Argo Steering Team*, 2009], which have sampled the Labrador Sea since the second half of the 1990s [*Lavender et al.*, 2002; *Våge et al.*, 2009]. The floats descend to a prescribed pressure level and move with the currents for a predefined number of days. They then ascend to the surface, while taking a CTD (conductivity, temperature and depth) profile. There are currently (January 2012) about 3000 autonomous floats in total spread over all ocean basins in the world, of which around

30 in the Labrador Sea. With a typical repeat cycle of 10 days in the Argo program these give around 300 profiles during the deep convection months of February to April.

The many in situ observations provide accurate and reliable information about the MLD at a certain location and a certain time, but they have a poor spatial and temporal coverage. As a result, there is not always a consensus on the depth of the mixed layer in a winter (see section 2 for an overview of convective activity since 1993). The one observational network that has none of these disadvantages is the satellite system: satellites are present throughout the year and sample the whole Labrador Sea. Although they cannot measure the MLD directly, they can measure the change in sea surface height (SSH) as a result of convective densification of the water column. During the deep convection season, the water density increases, causing a lowering of the sea level of several centimeters. The major part of this signal, however, is the seasonal cycle. To find out whether it is possible to detect deep convection, we should consider the additional cooling in a deep convection winter with respect to a shallow convection winter. If this additional cooling is about 0.2°C over 1500 meters [e.g. *Yashayaev and Loder*, 2009], and we assume a thermal expansion coefficient of 1×10^{-4} °C^{-1} [*Gelderloos et al.*, 2012, manuscript under review at the *Journal of Climate*], then the SSH is lowered by about

$$\Delta H = \int \alpha \Delta T dz \approx 3\text{cm}.$$

In this study the feasibility of detecting and monitoring the formation of Labrador Sea Water will be tested by comparing SSH fields (section 3) with the observed MLD over the past two decades, an overview of which is included in section 2. Using the SSH anomaly fields, we show in section 4 that it is possible to detect newly-formed LSW and also to give a very rough estimate of the convection depth and area. In section 5 we will take this one step further to try and link the MLD at a certain time and location to the SSH anomaly at that time and location, which we will show to be more challenging. The results are summarized in section 6.

2. Convective Activity in the Period 1993-2009

From the combined observational programs we have a reasonable idea of the interannual variability of deep convection in the Labrador Sea since the early 1990s (Table 1). The first years of this period were characterized by large winter heat losses and showed the deepest convection in the Labrador Sea on record [*Lazier et al.*, 2002; *Lilly et al.*, 2003; *Yashayaev*, 2007], with the deepest mixed layers reached between 1993 and 1995. From 1996 to 1999 the winter heat loss was moderate and so mixed layers decreased in depth, causing a multiyear period of restratification at middepth. Convection was generally around 1000 m in these years [*Lazier et al.*, 2002; *Lilly et al.*, 2003; *Avsic et al.*, 2006], although a local maximum MLD of 1500 m was recorded in 1997 during a wintertime survey [*Pickart et al.*, 2002]. This short revival is corroborated by the K1-mooring record, which showed a mixed layer of 1400 m in the 1997 winter. The winter of 2000 interrupted the restratification trend with another convection winter which formed a new class of LSW [*Yashayaev*, 2007]. Despite the fact that a new class was formed, the convection does not seem to have been very deep. *Yashayaev and Loder* [2009] cite a maximum MLD of 1300 m between 2000 and 2003, without being specific on the convection depth in 2000, while *Avsic et al.* [2006] suggest an MLD of 1100 m based on the mooring data. The same mooring record shows the deepest convection in the 2000-2003 period in 2003, with a maximum MLD of 1400 m. The period between 2004 and 2007 was reasonably quiet with convection not exceeding 700 to 1100 m [*Yashayaev and Loder*, 2009], although the mooring recorded an MLD of 1300 m in 2005 [*Avsic et al.*, 2006]. In 2008, deep convection returned with winter mixed layers of up to 1800 m depth [*Våge et al.*, 2009]. This seems so far to have been a single-year interruption of the long-term restratification period, however, as in 2009 and 2010 no deep convection has been observed.

Despite these complications, the combined database enables us to divide the winters into three categories: convection deeper than 1500 m (hereafter referred to as deep convection), convection to 1000 m or less (shallow convection), and convection between roughly 1000 m and 1500 m (intermediate convection). These depth limits may at first seem rather arbitrary, but they serve well as a first indication of the formation of LSW as summertime restratification typically reaches about 1000 m. Therefore, when convection is shallower than 1000 m, in general no renewal of LSW takes place.

From the overview in Table 1 it is clear that the exact depth of the mixed layer is not always agreed upon. This is not surprising, however, as the different observations where taken at different times and different locations (Figure 1). For example, the float profiles in the winter of 1996 are clustered around 58°N and 54°W, which is much further northwest than the AR7W line which the summer estimates are based on. Moreover, as noted by *Lazier et al.* [2002], internal waves and eddies can easily cause a difference of 100 m in the MLD between two measurements at different locations. Particularly large discrepancies are found in the MLD estimates for 1996, 1998, 2002 and 2005. We will come back to these years in section 4.5.

3. Sea Surface Height Anomaly Data: AVISO

The AVISO altimetry data center[1] provides maps of sea level anomaly on a high spatial resolution (1/3°) and interpolated to a daily temporal resolution. We used the 'updated' delayed time series for this study, which combines as many missions available at any given time and location to obtain the best possible quality of the SSH anomaly estimate (Table 2). The time series is over the period of October 1992 to January 2011.

The SSH time series display variability on different temporal and spatial scales. As the SSH signal related to a convective density change of the water column only explains a small part of the variability, filtering of the data is required. The filtering procedure is applied to every data point in the grid, but illustrated for the area-averaged time series in Figure 2.

One source of SSH variation is the long-term trend (Figure 2a). This is the result of changing thermohaline forcing over the center of the subpolar gyre and the subsequent warming since the 1990s. This has reduced the strength of the cyclonic gyre circulation and has resulted in a gyre-scale long-term positive trend in the SSH time series [*Häkkinen and Rhines*, 2004]. This trend is removed from the SSH fields by subtracting the one-year running mean from the original SSH time series at every grid point. The resulting detrended time series is shown as the dashed line in 2b.

Apart from the long-term trend a second gyre-scale source of variability is evident in the time series, which is the seasonal cycle (Figure 2b). This is caused in part by changes in the strength of the gyre circulation as a result of increasing and decreasing wind stress curl, and in part by thermohaline forcing, mainly surface heating and cooling. As our time series contains years with deep convection as well as shallow and intermediate convection, we expect the winter values from the mean seasonal cycle (solid line in Figure 2b) to be consistent with intermediately-deep mixed layers. We are thus interested in the deviation from the mean seasonal cycle, i.e. the difference between the dashed and the solid lines in

Figure 2, where we expect a large negative wintertime anomaly to be an indicator of deep convection. Note that the climatological fields were spatially smoothed in both directions with a one-degree boxcar filter.

The last form of variability is small-scale and not coherent in space or time. This noisy pattern of positive and negative SSH values is mainly caused by eddies. In particular the larger Irminger Rings (a typical radius of 25 km) have a non-negligible dynamical sea surface anomaly signal [$\mathcal{O}$(10cm); *Lilly et al.*, 2003]. The SSH values depend on the sense of rotation of the eddy, where anticyclonic eddies cause positive anomalies and cyclonic eddies negative anomalies.

The eddy-induced 'background noise' is removed from the fields by averaging over time and over subregions of the Labrador Sea (see section 4 for details). This procedure is justified for our purposes, because deep convective mixing takes place in convective plumes on a very small horizontal scale of about 1 km, but during convection as well as directly following the event, violent lateral mixing homogenizes nearby plumes with the more stratified water in between into a homogeneous dense mixed patch or 'chimney', typically tens of kilometers to more than 100 km in diameter [*Marshall and Schott*, 1999]. It is therefore not necessary to catch the individual plumes in order to be able to detect deep convection. It is sufficient to detect the chimneys. Note that the chimneys are also much larger than eddies so that the two features can easily be distinguished in an SSH anomaly map.

4. Detecting Newly-Formed Labrador Sea Water Using Altimetry

4.1. Visual Inspection: Detecting the Chimney

As a first indication whether or not deep convection occurred in a winter, we take a look at the winter-mean (February-April) values of the SSH anomaly fields to see if the chimneys are visible. If so, they should show up as a relatively large area of strongly negative SSH anomalies. A map of the SSH anomaly in the only deep-convection winter of the past decade (2008) immediately reveals the deep convection area (Figure 3a) as a large dark blue patch of negative SSH anomalies larger than -2.5 cm, roughly between 56-59°N and 55-50°W. The deep convection site is surrounded by a noisy pattern of positive and negative anomalies of slightly smaller amplitude, which is caused by eddies in the basin. The same map for the winter of 2009, in contrast, only shows this noisy pattern and has no large-scale coherent negative anomaly. This is consistent with the fact that 2009 was a known shallow-convection winter (according to our definition in section 2; Table 1).

4.2. Time and Space-Averaged SSH Anomalies

Based on the example in Figure 3 one would expect that the mean SSH anomalies in a deep convection winter, if averaged over a suitably chosen area, will be significantly more negative than in shallow convection winters. This is shown in Figure 4 for the rectangular areas highlighted in Figure 1, averaged over February and March (solid squares) and February to April (open squares). The known deep convection winters (1994, 1995, and 2008) generally stand out by their large negative SSH anomaly. Also, well-known shallow-convection years (e.g. 1999 and 2001) clearly show a positive anomaly. Note that due to larger eddy activity in the northern part of the Labrador Sea [*Lilly et al.*, 2003, their Figure 24], the SSH anomalies averaged over the northwesternmost box (Figure 4d) are smaller than in the other boxes; i.e. the convective signal is smaller due to more eddy noise.

Convection of intermediate depth is more difficult to diagnose, partly because the winter-mean anomaly depends on the area over which the average is taken. For example, in the small rectangular domain in the southwestern part of the Labrador Sea (Figure 4e) the negative SSH anomaly in 1997 was much larger than in 2000, while the averages over the large rectangular area, representative for the southern Labrador Sea (Figure 4a), show comparable anomalies. Apparently, the MLD was large in the southwest corner of the Labrador Sea in 1997, but averaged over the larger domain a similar densification has taken place.

The differences between the different areas can also be used to locate the area of deepest convection. 1997 is a very good example: The deepest convection was in the southwestern corner [*Pickart et al.*, 2002], which is reflected in the relatively large negative anomaly in 1997 in Figure 4e with respect to the other panels. 2008 also shows that it is useful to look at different areas. Due to the large sea-ice extent in the winter of 2008, the deep convection was slightly more southwards and eastwards than usual. Therefore, the negative SSH anomaly in the eastern and southern areas are larger than in the western and northwestern areas.

Two winters, 2003 and 2006, show unsatisfying results. According to in situ measurements (Table 1), 2003 was an intermediate convection winter, but the SSH anomaly is surprisingly positive. In contrast, the evidence suggests 2006 to have been a shallow convection winter, yet in this year a negative wintertime SSH anomaly is observed. Both of these cases seem to be independent of the area over which is averaged (Figure 4). We will get back to these winters when looking at the time dependency of the SSH anomaly (sections 4.3 and 4.4).

In summary, using straightforward temporal and spatial averaging, only 2 out of 17 winters show results inconsistent with *in situ* observations. Furthermore, all three deep convection winters are easily identified.

4.3. Time-Dependent SSH Anomalies

The Hovmöller diagrams in Figure 5 show the latitude and time variation of the SSH anomalies in the southwestern part of the Labrador Sea (cf. Figure 4b). The deep convection winters, indicated by a solid rectangle surrounding the panel of that year, clearly show prolonged and coherent negative anomalies. This is particularly true for 1994 and 2008. 1995 also shows a large-scale prolonged negative anomaly, but only until mid-March rather than mid-April, after which the signal is more variable. This very nicely reflects the fact that the winter of 1995 was not a particularly harsh one [*Uppala et al.*, 2005]; the convection was mainly so deep because this winter was preceded by a deep convection period lasting multiple winters in a row. Apparently, there was deep convection in February, but no more convective densification in March and April than in an average winter.

The intermediate convection winters (1997, 2000 and 2003; indicated by a dashed frame in Figure 5) are characterized by negative anomalies of a similar latitudinal extent and amplitude as in the deep convection winters, but of shorter duration. The reason for the seemingly very large positive SSH anomaly in 2003 in Figure 4 now immediately becomes clear: it originates from a very high positive anomaly in the first half of February. The SSH anomaly during the rest of the winter is comparable to, for example, 2000. In this case, it is thus very important to look at the time evolution of the SSH anomaly before drawing conclusions: from mid February onwards 2003 was definitely an intermediate-convection winter, in line with the conclusions from in situ observations (Table 1).

Four of the six shallow convection winters (no frame; 1999, 2001, 2004 and 2009) show only weak negative anomalies (fade shades of blue) or positive values (red and pink shades), as expected. The other two shallow convection winters, 2006 and 2007, can be classified as either shallow or intermediate convection winters, based on a comparison with the other panels in Figure 5.

Out of the 12 winters under consideration that have an undisputed convective regime (see Table 1), there are thus only 2 winters that are classified as shallow based on the *in situ* observations for which the SSH anomaly analysis suggests a different convective regime (intermediate). These winters, 2006 and 2007, are examined below.

4.4. When Altimetry Seems to Fail: 2006 and 2007

For the winter of 2007 the explanation for the discrepancy between the altimetric SSH anomaly and the in situ-measured MLD is straightforward. In February and early March of that year, the entire gyre was lower than average (Figure 6a), in contrast to a chimney-like feature in a deep convection year (see Figure 3a). At the same time, an exceptionally large wind stress curl is observed around the southern tip of Greenland and spread over the Irminger Sea and the southern part of the Labrador Sea (Figure 6b). It can be expected that such a large wind stress spins up the cyclonic circulation of the gyre, yielding a negative SSH anomaly over a large area, consistent with the observations. The large negative SSH anomaly in 2007 is thus a wind effect and not the result of convective densification. This type of results is thus easily eliminated by considering a larger area and looking at the wind fields.

Explaining the negative anomaly in the winter of 2006 is more difficult. In the monthly-mean SSH anomaly maps (Figure 7), only in February two chimney-like features can be discerned. The floats showed no deep mixed layers in the 'chimney' around 60°N and 53°W. At the location of the second chimney-like feature, centered around 57°N and 52°W, the profiling floats recorded mixed layers around 800 m. The fact that the SSH anomalies in March and April are comparable to normal values for the time of the year also indicates that, if convection took place in February, it did not reach very deep. This is confirmed by the lack of newly-formed deep water on the AR7W line in spring. One possible explanation is that the dip in sea level is not a chimney, but a cluster of cyclonic eddies which all remain fairly stable at the same position during the month of February. This is not very likely, however, as the larger eddies in the Labrador Sea are predominantly anticyclonic [*Lilly et al.*, 2003]. Another possibility is that an increased wind stress curl over the Irminger Sea, East of Greenland [known as a Greenland tip jet; *Doyle and Shapiro*, 1999; *Pickart et al.*, 2003], induced a cyclonic recirculation gyre extending into the Labrador Sea as described by *Spall and Pickart* [2003]. Indeed, according to the wind stress data from the ERA-interim reanalysis a number of high wind stress curl events occurred in this region between late January and halfway March [*Dee et al.*, 2011]. As the increased wind stress curl events were local, a spinup of the entire gyre such as in 2007 would not have occurred. Nevertheless, as for 2007, we suspect that local wind effects played a role in lowering the sea surface in this winter.

4.5. When In Situ Monitoring Programs Disagree: 1996, 1998, 2002 and 2005

As discussed in section 2, for four winters in the past two decades the in situ observations disagree on whether the convective regime was shallow or intermediate. These winters are indicated by a dash-dotted frame in Figure 5. With the knowledge from the analyses of the SSH anomalies of all winters we can now estimate the convective regime in these winters. Both 1998 and 2002 show coherent negative anomalies in the Hovmöller plots (Figure 5) during March and April, such as can be found in 1997 and 2000. The timing and spatial extent of these negative anomalies indicate that these two years had an intermediate convection regime, consistent with the moderate negative winter-mean SSH anomalies in these two years (Figure 4).

In contrast, the Hovmöller diagrams of 1996 and 2005 show mainly positive and very weak anomalies, the only exception being the second half of April 2005. This negative anomaly, however, does not appear to represent one but two features, the size of which resemble the dimensions of an eddy rather than those of a chimney. Furthermore, the anomaly is very late in the convection season, as convective densification is typically largest in February and March. Overall, the winter-mean SSH anomalies in 1996 and 2005 were large and positive, indicating that these years likely had a shallow-convection regime. The SSH anomaly fields can thus successfully help solve the disagreement between *in situ* observations.

5. Potential of Altimetry as a Monitoring Tool

In the previous section we showed that, by averaging the satellite altimetry data in several different ways and careful consideration of the resulting patterns and evolution, winters can be classified as deep, intermediate and shallow convective regimes (Figures 4 and 5). Also, the area where convective densification has taken place can roughly be located (Figure 3a). A more ambitious goal is to not only *detect* newly-formed deep water using satellite altimetry, but to use it as an operational tool to *monitor* where and when deep convection takes place in the Labrador Sea. The difficulty here is that the signal of convection in the SSH anomaly fields (a range of about 4 cm, see Figure 4) is typically smaller than the (mostly eddy-induced) background noise. The averaging procedures in section 4 suppress the noise, which makes detection feasible.

To be able to operationally monitor LSW formation with satellite altimetry, a tight relation between the *local* SSH anomaly measured by the altimeter and the *local* depth of the mixed layer must exist, without averaging in time and space. In this section we will test this relation by correlating in situ-measured MLDs with the SSH anomalies measured by the altimeter. The MLDs are derived from float profiles obtained between 1996 and 2009, and the stations from the winter cruise in February/March 1997 [*Pickart et al.*, 2002]. The procedure for deriving the MLDs is explained in section 5.1. Then the correlation between SSH anomaly and the depth of the mixed layer is studied in section 5.2.

5.1. Float-Based Mixed Layer Depth

As part of the World Ocean Circulation Experiment (WOCE), the Labrador Sea Deep Convection Experiment and later as part of the Argo program the interior Labrador Sea has been sampled by autonomous profiling floats [*LabSeaGroup*, 1998; *Lavender et al.*, 2000; *Straneo*, 2006; *Våge et al.*, 2009]. The floats give information on the temperature and salinity distribution, from which the depth of convection in winter can be derived. From 1997 to 1999 and from 2005 to 2009 the spatial coverage during the deep convection season (February to April) is rather good (typically 50 to 150 profiles per winter, with a fair coverage of the central Labrador Sea). Some profiles are available as well for the winters of 1996 and 2000 to 2004 (typically 10 to 50 profiles per winter, with only a limited spatial coverage). Figures 8a and b show an example of a poorly sampled winter and a well sampled winter, respectively. A complete overview of the number of floats per winter is given in Table 3. A total number of 1104 profiles were included in the analysis.

Pickart et al. [2002] determined the MLD from the stations during the winter cruise in 1997 as follows. First, a subjective estimate of the MLD was made by visual inspection of the potential density profile. Then, the mean density and the standard deviation were computed over the depth range of the subjectively estimated MLD. The two-standard deviation envelope was then overlaid on the potential density profile and the MLD was determined as the depth where the profile permanently crossed outside of this envelope. In a later study, *Våge et al.* [2009] used the same method to determine the mixed layer depth (MLD) of the floats in the Labrador Sea that were part of the Argo program (winter data in the Labrador Sea in 2002-2009). Here we expand the MLD record using the floats deployed as part of WOCE and the Labrador Sea Deep Convection Experiment [*Lavender et al.*, 2005], which provided winter profiles in the Labrador Sea between 1996 and 2001.

Before comparing the in situ-measured MLDs with the altimetry-derived SSH anomaly, an additional step had to be taken. The spatial spreading of the float profiles is always different. This is especially a problem when a float is trapped inside a cyclonic eddy, because this links the MLD in the eddy (which need not be large) to the large negative SSH anomaly of the eddy. To avoid these (and other) spurious matches from dominating the overall correlation between the MLD and SSH anomaly, we interpolated the in situ measured MLDs onto the same grid as the SSH anomaly fields to obtain MLD maps

(Figures 8c and d). For this interpolation an optimum had to be found between a minimum of temporal averaging (as too much averaging would be useless from an operational point of view) and a minimum distance between floats used for the interpolation (as large distances make the interpolated map unreliable). Based on a subjective evaluation, we found that a month was the minimum time period required to have enough profiles to make a map. Naturally, these maps do still not cover the entire Labrador Sea and also in the area we use for the analysis 'white spots' remain, i.e. grid points too far away from the nearest float or CTD station (white areas in Figures 8c and d). After making the maps, the SSH anomaly maps (Figures 8e and f) are subsampled on the valid data points from the MLD maps, i.e. the areas not covered by 'white spots', for further analysis.

5.2. Relating SSH Anomaly to Mixed Layer Depth

First, every valid grid point (non-white grid points in Figures 8c and d, and equivalent for all other years and months) of the MLD maps were plotted against the accompanying SSH anomaly (Figures 8e and f). The result is shown in Figure 9a. The correlation between the SSH anomaly and the MLD is -0.26 (p value = 0.00, 1896 data points). This means in physical terms, which is also immediately clear from the figure, that the local SSH anomaly is not a good indicator for the local MLD in a certain month. Apparently, the averaging procedures from section 4 are indeed necessary to separate the convective densification signal from the eddy-induced variability. This is shown in Figure 9b. Here, the valid points from the maps like Figure 8c and d are averaged over the southwesternmost box from Figure 1 in the Labrador Sea (area indicated in Figure 8) and compared to the accompanying averaged SSH anomaly value. This increases the correlation to -0.4 (p value = 0.01, 41 data points). This is still not sufficient, however, to be able to use the altimeter for operational monitoring purposes. Averaging to suppress small scale variability and a certain amount of expert judgment (section 4) are required to determine the convective regime.

6. Summary and Conclusions

From the combination of the winter-mean sea surface height (SSH) anomalies (Figure 4) and Hovmöller diagrams of these SSH anomalies (Figure 5) we have shown that it is possible to detect newly-formed Labrador Sea Water (LSW) from altimetry data and to estimate whether the wintertime mixed layer depths (MLDs) from 1994 to 2009 were deep (>1500 m), shallow (< 1000 m), or intermediate (between roughly 1100 and 1400 m). The reason we make the distinction between shallow and intermediate convection is because most of the literature on deep convection is in terms of MLD, while the altimetry measures the change in density[2]. These are, of course, strongly related, but a winter following a restratification period of multiple years requires a larger densification of the water column to mix convectively to a certain depth. It is therefore useful to make a distinction between convection which can produce a traceable amount of LSW (the intermediate convection winters in our study), and that which can not (shallow convection).

The most interesting winters are the deep convection winters, which ventilate the deeper layers of the Labrador Sea. These winters can be easily and irrefutably singled out based on satellite altimetry data alone. Most of the intermediate and shallow convection winters are easily identified as well. For some winters, however, spatial maps and expert judgment are required to draw the correct conclusion. In one winter, the winter of 2006, all analyses of the SSH anomaly suggest an intermediate convection winter, while no such convection has been reported from in situ measurements. For all other winters, however, the SSH anomaly fields were consistent with the in situ-measured MLD.

In an earlier study *Herrmann et al.* [2009] suggested the possibility to monitor deep convection in the northwestern Mediterranean Sea using satellite altimetry. Their study is based on the same basic concept as ours, but differs on some essential points. In particular, *Herrmann et al.* [2009] used a model hindcast to find a (linear) relation between deep convection and the local SSH anomaly. Assuming this relation would hold for the observations in the real ocean as well, they estimated the MLD based on satellite altimetry data. However, it appears that this relation does not always hold, not even in their model simulations (see for example the large negative anomalies north of point 'B' in the lower panel of their Figure 1e, which do not correspond to a deep mixed layer). Furthermore, it is assumed that the location of the deepest mixed layer in the model is exactly the same as in reality. Certainly in the Labrador Sea, there is quite some variability in the location where the deepest convection occurs [*Våge et al.*, 2009]. We found no simple linear relationship between the local MLD and local SSH anomaly in the Labrador Sea. Detection of newly-formed LSW is only possible if spatial and temporal averaging is applied first. Therefore, satellite altimetry can not be used to monitor the formation of LSW for operational purposes, and the approach of *Herrmann et al.* [2009] will not provide reliable results in the Labrador Sea case. We note that inclusion of concurrent wind stress curl measurements, and perhaps SST and SSS, could add to the detection algorithm. This is however beyond the scope of this altimetry study.

We have shown that satellite altimetry can be used successfully to detect newly formed deep water and roughly indicate the location. This does not mean that in situ measurements have become superfluous, and conclusions based on altimetry need to be interpreted with care. The major advantage of using satellites for the detection of deep convection is their high temporal resolution and large spatial coverage, which enable detecting the occurrence of deep water formation away from the annual hydrographic repeat section. This information can be used to guide research vessels. When applied in this way, satellite altimetry is thus a very useful and valuable addition to the efforts to monitor variability in deep water formation in the Labrador Sea.

Acknowledgments. This research was funded by a grant from the NWO/SRON User Support Programme Space Research. The altimeter products were produced by Ssalto/Duacs and distributed by Aviso, with support from Cnes (http://www.aviso.oceanobs.com/duacs/). We are grateful to Robert Pickart for supplying his mixed layer depth estimates from the 1997 winter hydrographic survey and to Fiamma Straneo and Tatiana Rykova for providing float profiles for the pre-Argo period.

Notes

1. http://www.aviso.oceanobs.com/en/data/products/sea-surface-height-products/global/msla/index.html#c5122
2. Relating the change in density from altimetry measurements to formation rates such as in *Rhein et al.* [2011] may be a more appropriate comparison, but unfortunately these formation rates are only available per two years and not per year.

References

AVISO 2011 (2011), *SSALTO/DUACS user handbook: (M)SLA and (M)ADT near-real time and delayed time products*, AVISO, 2rev 6 ed., reference: CLS-DOS-NT-06-034.

Avsic, T., J. Karstensen, U. Send, and J. Fischer (2006), Interannual variability of newly formed Labrador Sea Water from 1994 to 2005, *Geophysical Research Letters*, *33*, L21S02, doi:10.1029/2006GL026913.

Biastoch, A., C. Böning, and J. Getzlaff (2008), Causes of interannual-decadal variability in the meridional overturning circulation of the midlatitude North Atlantic Ocean, *Journal of climate*, *21*, 6599–6615.

Bower, A., M. Lozier, S. Gary, and C. Böning (2009), Interior pathways of the North Atlantic meridional overturning circulation, *Nature*, *459*, 243–248, doi: 10.1038/nature07979.

Dee, D. P., S. M. Uppala, A. J. Simmons, P. Berrisford, P. Poli, S. Kobayashi, U. Andrae, M. A. Balmaseda, G. Balsamo, P. Bauer, P. Bechtold, A. C. M. Beljaars, L. van de Berg, J. Bidlot, N. Bormann, C. Delsol, R. Dragani, M. Fuentes, A. J. Geer, L. Haimberger, S. B. Healy, H. Hersbach, E. V. Hólm, L. Isaksen, P. Kållberg, M. Köhler, M. Matricardi, A. P. McNally, B. M. Monge-Sanz, J.-J. Morcrette, B.-K. Park, C. Peubey, P. de Rosnay, C. Tavolato, J.-N. Thépaut, and F. Vitart (2011), The era-interim reanalysis: Configuration and performance of the data assimilation system, *Quart. J. Roy. Meteor. Soc.*, *137*(656), 553–597, doi:10.1002/qj.828.

Doyle, J. D., and M. A. Shapiro (1999), Flow response to large-scale topography: the Greenland tip jet, *Tellus*, *51A*, 728–748.

Eden, C., and J. Willebrand (2001), Mechanism of interannual to decadal variability of the North Atlantic circulation, *Journal of Climate*, *14*, 2266–2280.

Gelderloos, R., F. Straneo, and C. A. Katsman (2012), Mechanisms behind the temporary shutdown of deep convection in the Labrador Sea: Lessons from the Great Salinity Anomaly years 1968-1971, *under review at Journal of Climate*.

Häkkinen, S., and P. B. Rhines (2004), Decline of the subpolar North Atlantic circulation during the 1990s, *Science*, *304*, 555–559.

Herrmann, M., J. Bouffard, and K. Béranger (2009), Monitoring open-ocean deep convection from space, *Geophysical Research Letters*, *36*, L03606, doi:10.1029/2008GL036422.

Kuhlbrodt, T., A. Griesel, M. Montoya, A. Levermann, M. Hofmann, and S. Rahmstorf (2007), On the driving processes of the Atlantic meridional overturning circulation, *Reviews of Geophysics*, *45*, RG2001, doi:10.1029/2004RG000166.

LabSeaGroup (1998), The Labrador Sea deep convection experiment, *Bulletin of the American Meteorological Society*, *79*, 2033–2058.

Lavender, K. L., R. E. Davis, and W. B. Owens (2000), Mid-depth recirculation observed in the interior Labrador and Irminger Seas by direct velocity measurements, *Nature*, *407*, 66–69.

Lavender, K. L., R. E. Davis, and W. B. Owens (2002), Observations of open-ocean deep convection in the Labrador Sea from subsurface floats, *Journal of Physical Oceanography*, *32*, 511–526.

Lavender, K. L., W. B. Owens, and R. E. Davis (2005), The mid-depth circulation of the subpolar North Atlantic Ocean as measured by subsurface floats, *Deep-Sea Research I*, *52*, 767–785.

Lazier, J. (1980), Oceanographic conditions at ocean weather ship Bravo, 1964-1974, *Atmosphere-Ocean*, *18*, 227–238.

Lazier, J., R. Hendry, A. Clarke, I. Yashayaev, and P. Rhines (2002), Convection and restratification in the Labrador Sea, *Deep-Sea Research I*, *49*, 1819–1835.

Lilly, J., P. Rhines, R. Davis, J. Lazier, F. Schott, and D. Farmer (1999), Observing deep convection in the Labrador Sea during winter 1994/95, *Journal of Physical Oceanography*, *29*, 2065–2098.

Lilly, J., P. Rhines, F. Schott, K. Lavender, J. Lazier, U. Send, and E. D'Asaro (2003), Observations of the Labrador Sea eddy field, *Progress in Oceanography*, *59*, 75–176.

Marshall, J., and F. Schott (1999), Open-ocean convection: Observations, theory, and models, *Review of Geophysics*, *37*, 1–64.

Pickart, R. S., D. J. Torres, and R. A. Clarke (2002), Hydrography of the Labrador Sea during active convection, *Journal of Physical Oceanography*, *32*, 428–457.

Pickart, R. S., M. A. Spall, M. H. Ribergaard, G. W. K. Moore, and R. F. Milliff (2003), Deep convection in the Irminger Sea forced by the Greenland tip jet, *Nature*, *424*, 152–156.

Rhein, M., D. Kieke, S. Hüttl-Kabus, A. Roessler, C. Mertens, R. Meissner, B. Klein, C. W. Böning and I. Yashayeav (2011), Deep water formation,the subpolar gyre,and the meridional overturning circulation in the subpolar North Atlantic, *Deep-Sea Research II*, *58*, 1819–1832.

Roemmich, D., G. C. Johnson, S. Riser, R. Davis, J. Gilson, W. B. Owens, S. L. Garzoli, S. Schmid, and M. Ignaszewski (2009), The Argo program: Observing the global ocean with profiling floats, *Oceanography*, *22*, 34–43, doi:10.5670/oceanog.2009.36.

Roemmich, D. and the Argo Steering Team (2009), The challenge of continuing 10 years of progress, *Oceanography*, *22*, 46–55, doi:10.5670/oceanog.2009.65.

Spall, M. A., and R. S. Pickart (2003), Wind-driven recirculations and exchange in the Labrador and Irminger Seas, *Journal of Physical Oceanography*, *33*, 1829–1845.

Straneo, F. (2006), Heat and freshwater transport through the central Labrador Sea, *Journal of Physical Oceanography*, *36*, 606–628.

Talley, L. D., and M. S. McCartney (1982), Distribution and circulation of Labrador Sea Water, *Journal of Physical Oceanography*, *12*, 1189–1205.

Uppala, S. M., P. W. Kallberg, A. J. Simmons, U. Andrae, V. da Costa Bechtold, M. Fiorino, J. K. Gibson, J. Haseler, A. Hernandez, G. A. Kelly, X. Li, K. Onogi, S. Saarinen, N. Sokka, R. P. Allan, E. Andersson, K. Arpe, M. A. Balmaseda, A. C. M. Beljaars, L. van de Berg, J. Bidlot, N. Bormann, S. Caires, F. Chevallier, A. Dethof, M. Dragosavac, M. Fisher, M. Fuentes, S. Hagemannn, E. Holm, B. J. Hoskins, L. Isaksen, P. A. E. M. Janssen, R. Jenne, A. P. McNally, J. F. Mahfouf, J. J. Morcrette, N. A. Rayner, R. W. Saunders, P. Simon, A. Sterl, K. E. Trenberth, A. Untch, D. Vasiljevic, P. Viterbo, and J. Woollen (2005), The ERA-40 re-analysis, *Quarterly Journal of the Royal Meteorological Society*, *131*, 2961–3012.

Våge, K., R. Pickart, V. Thierry, G. Reverdin, C. Lee, B. Petrie, T. Agnew, A. Wong, and M. Ribergaard (2009), Surprising return of deep convection to the subpolar North Atlantic Ocean in winter 2007-2008, *Nature Geoscience*, *2*, 67–72.

Yashayaev, I. (2007), Hydrographic changes in the Labrador Sea, 1960-2005, *Progress in Oceanography*, *73*, 242–276.

Yashayaev, I., and J. Loder (2009), Enhanced production of Labrador Sea Water in 2008, *Geophysical Research Letters*, *36*, doi:10.1029/2008GL036162.

Year	AR7W Y09	AR7W L03	AR7W L02	AR7W P02	K1 A06	Floats A06	Floats Y09	Floats V09/GKV12
1993	2400	2300	2320	-	-	-	-	-
1994	-	2000	2300	-	-	-	-	-
1995	-	2300	-	-	2300	-	-	-
1996	-	1200	$\leq$1000	-	-	1300	-	630
1997	-	1400	$\leq$1000	1500	1400	-	-	1420
1998	-	1000	$\leq$1000	-	1000	-	-	1170
1999	-	900	$\leq$1000	-	1000	-	-	1040
2000	*	-	-	-	1100	-	-	1020
2001	1300	-	-	-	1100	-	700 -	900
2002		-	-	-	1200	-	1100	690
2003		-	-	-	1400	-	1200-1300	1330
2004	-	-	-	-	-	700		820
2005	-	-	-	-	1300	-	700 -	1290***
2006	-	-	-	-	-	-	1100	990
2007	<700	-	-	-	-	-		940
2008	1600	-	-	-	-	-	1600**	1830
2009	-	-	-	-	-	-	-	790

Table 1. Compilation of estimates of maximum winter MLD in the Labrador Sea for 1993-2009 from various locations and sources (gray shading marks the deep convection years, dashes indicate no specific estimate in that manuscript). The estimates in the first three columns are based on summertime surveys of the AR7W section (Y09: *Yashayaev and Loder* [2009]; L03: *Lilly et al.* [2003]; L02: *Lazier et al.* [2002]). Other columns represent wintertime measurements from the 1997 winter survey (P02: *Pickart et al.* [2002]), the K1 mooring (A06: *Avsic et al.* [2006]), and float data (A06: profiles obtained near the K1 mooring + some summertime CTD stations; Y09: rough estimate for the central Labrador Sea). The final column contains estimates based on a detailed analysis of available float profiles for 1996–2001 (section 5.1, denoted in the table as GKV12) and 2002–2009 [V09: *Våge et al.*, 2009]:. **Yashayaev* [2007] states that wintertime convection in 2000 reached 1600 m. ***Yashayaev and Loder* [2009] note that one float suggested an MLD greater than 1800 m. ***The deep mixed layer in 2005 was located just southwest of the Greenland coast.

Period	Missions used
October 1992 to August 2002	Topex/Poseidon + ERS-1 or ERS-2
August 2002 to June 2003	Jason-1 + ERS-2
June 2003 to January 2004	Jason-1 + Envisat
From January 2009	OSTM/Jason-2 + Envisat

Table 2. Satellite missions used in the AVISO merged altimetry product [AVISO 2011].

Year	# Float profiles			
	Feb	Mar	Apr	Total
1996	3	4	3	10
1997	19	20	12	51
1998	55	70	58	183
1999	21	17	15	53
2000	8	6	6	20
2001	3	3	3	9
2002	1	4	6	11
2003	18	31	26	75
2004	20	21	18	59
2005	34	36	33	103
2006	35	47	42	124
2007	52	54	53	159
2008	31	37	35	103
2009	35	29	27	91

Table 3. Number of float profiles in the area between 65-42°W and 52-65°N (Figure 8a and b), per year per month.

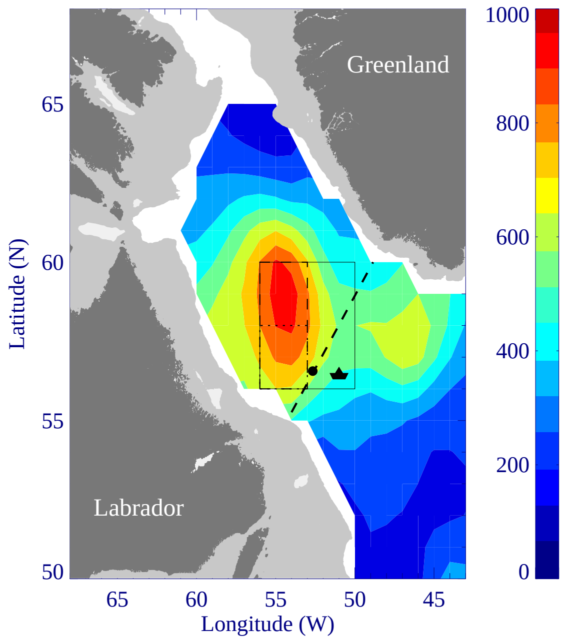

Figure 1. Overview of the locations of repeated measurements (the 2000-2007 mixed layer depth climatology from *Våge et al.* [2009] is shown in color). The dashed line across the basin is the AR7W hydrographic repeat section. The little boat is the location of Ocean Weather Station Bravo, and the black dot on the AR7W line close to Bravo is the location of the K1 mooring (see Table 1 for an overview of the mixed layer depths measured at these locations since 1993). The solid, dashed and dotted rectangles are the areas over which is averaged in sections 4 and 5. Areas shallower than 500 m are shaded in pale gray.

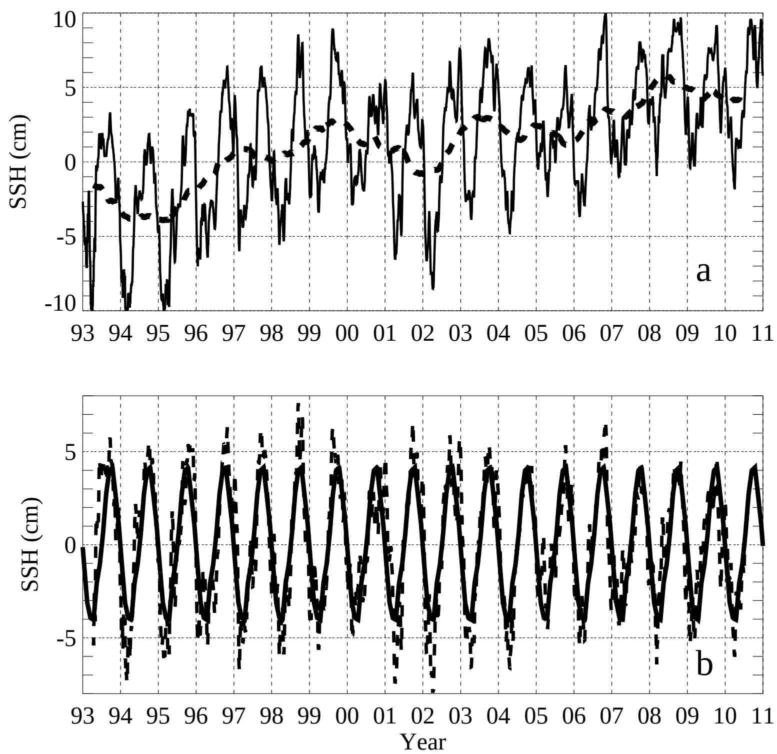

Figure 2. Filtering of the original SSH data to obtain the SSH anomaly (all time series are the average over 56-60°N and 56-53°W, the large rectangle in Figure 1). (a) Original time series (solid line) with the 1-year running mean overlaid (dashed line). (b) Detrended time series: The dashed line is the difference between the two timeseries in panel a. The solid line is the mean seasonal cycle of the detrended time series. The analysis is performed on the difference between the detrended time series (dashed line in panel b) and the mean seasonal cycle (solid line in panel b). This quantity will be called 'SSH anomaly'. Note that the area-averaged time series shown in this figure only serve to explain the filtering method used. In the analysis the filtering is performed on each data point in the grid individually.

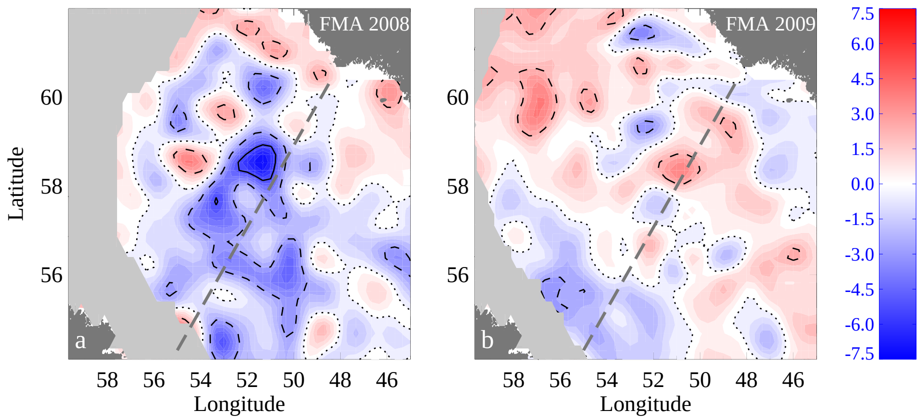

Figure 3. SSH anomaly (SSH minus long-term trend minus the mean seasonal cycle; see text in section 3) in cm, averaged over February to April. (a) A deep convection winter (2008) and (b) a shallow convection winter (2009). Greenland (in the northeast) and Labrador (in the southwest) are indicated in dark gray. The AR7W hydrographic section is added for reference as the thick gray dashed line from Labrador to Greenland. The zero-contour is dotted, the -2.5 and +2.5 cm contours are dashed, and the -5 and +5 cm contours are indicated by a solid black line. The pale gray shading indicates where the AVHRR-measured March-mean sea ice concentration was more than 50%.

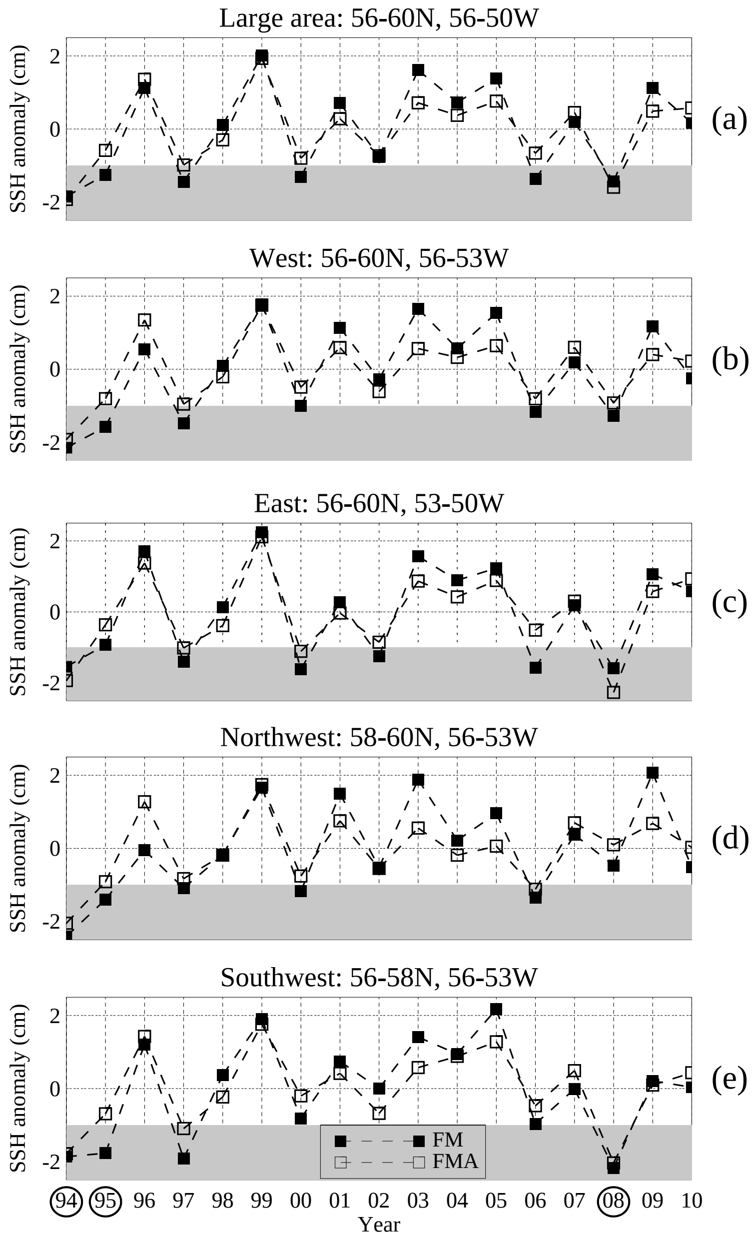

Figure 4. Multimonth mean SSH anomaly per year averaged over (a) 56-60°N and 56-50°W (the large, solid rectangle in Figure 1); (b) 56-60°N and 56-53°W (the western half of the solid rectangle; the 53°W line is indicated in Figure 1 by the dashed line); (c) 56-60°N and 53-50°W (the eastern half of the solid rectangle); (d) 58-60°N and 56-53°W (the northwestern part of the solid rectangle; the 58°N line is indicated in Figure 1 by the dotted line); (e) 56-58°N and 56-53°W (the southwestern part of the solid rectangle). Negative SSH anomalies larger than -1 cm are shaded to help visual inspection. Deep convection winters (MLD > 1500 m) are highlighted by a circle around the year on the x-axis. Note that we lost one year of data on both sides of the time series due to subtraction of the one-year running mean.

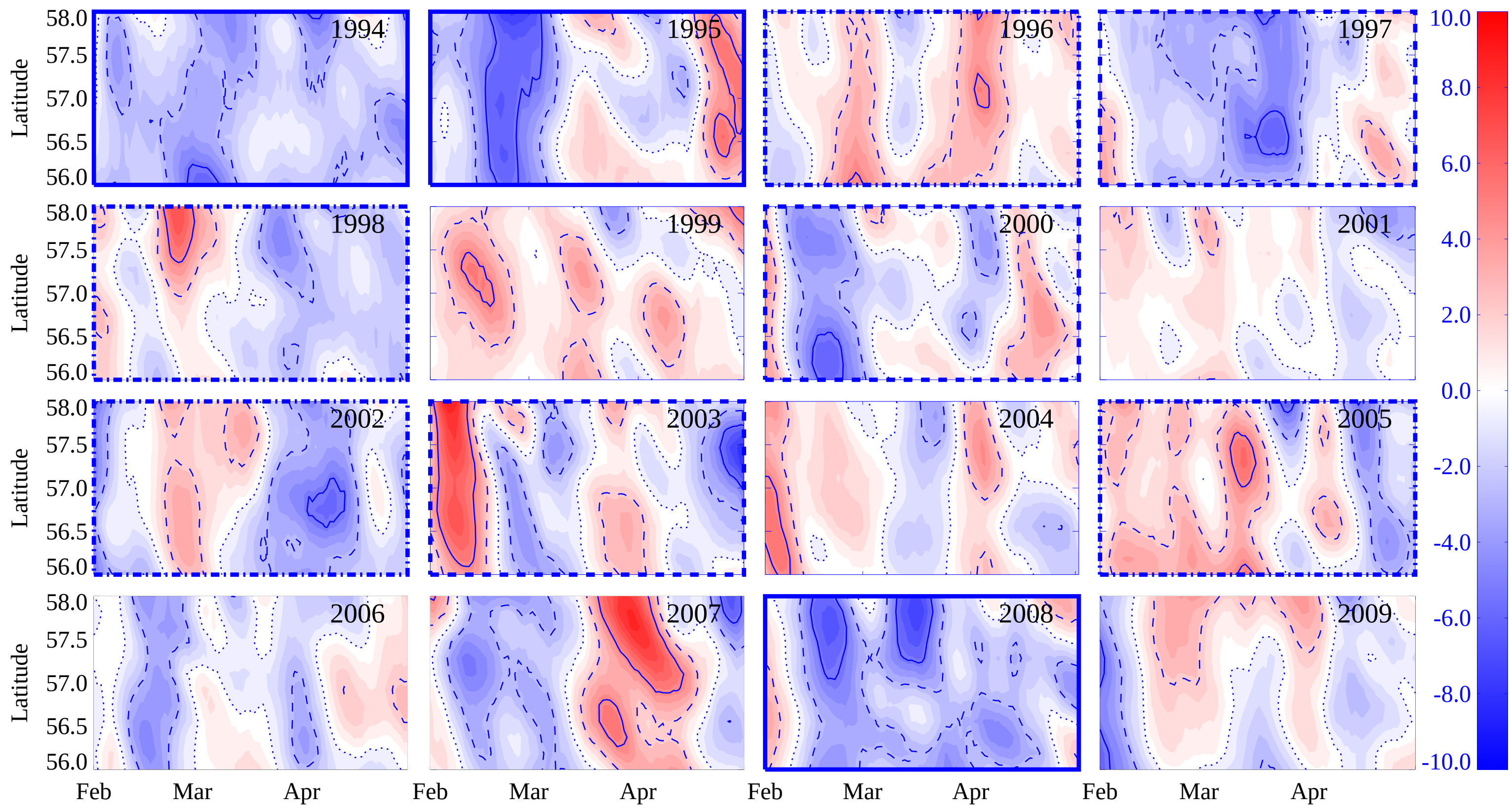

Figure 5. Hovmöller plots of the SSH anomaly (cm) for 1994 to 2009, zonally averaged over 56-53°W (small rectangle in Figure 1). Winters with deep convection are surrounded by a thick solid frame, intermediate-convection winters are indicated by a dashed frame, and shallow-convection winters have no frame. The four winters on which literature is not conclusive whether intermediate of shallow convection took place have a dash-dotted frame. The contour levels are as in Figure 3.

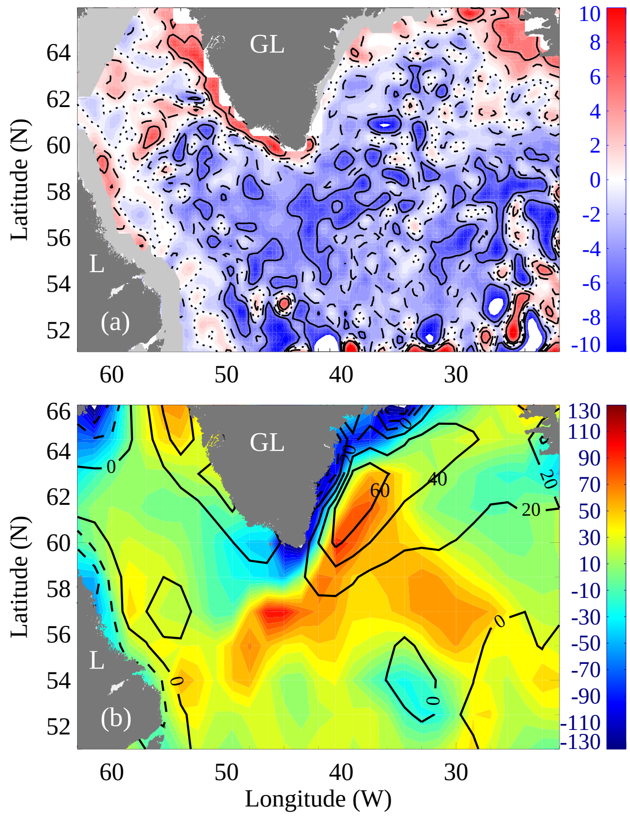

Figure 6. (a) February-mean SSH anomaly in 2007. The pale gray shading indicates where the AVHRR-measured February-mean sea ice concentration was more than 50%. (b) Wind stress curl fields (N/m$^3 \times 10^{-8}$) calculated from the ERAinterim time series [*Dee et al.*, 2011]. In color is the mean wind stress curl over February 2007. The climatological February wind stress curl over 1993 to 2009 is overlaid in contour lines. GL = Greenland; L = Labrador.

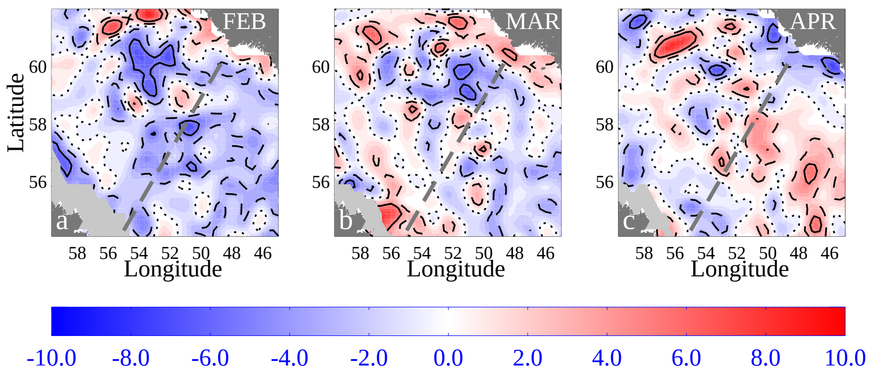

Figure 7. Monthly-mean SSH anomaly maps of 2006. (a) February; (b) March; (c) April. The continents, AR7W line and contours are as in Figure 3. The pale gray shading indicates where the AVHRR-measured monthly mean sea ice concentration was more than 50%.

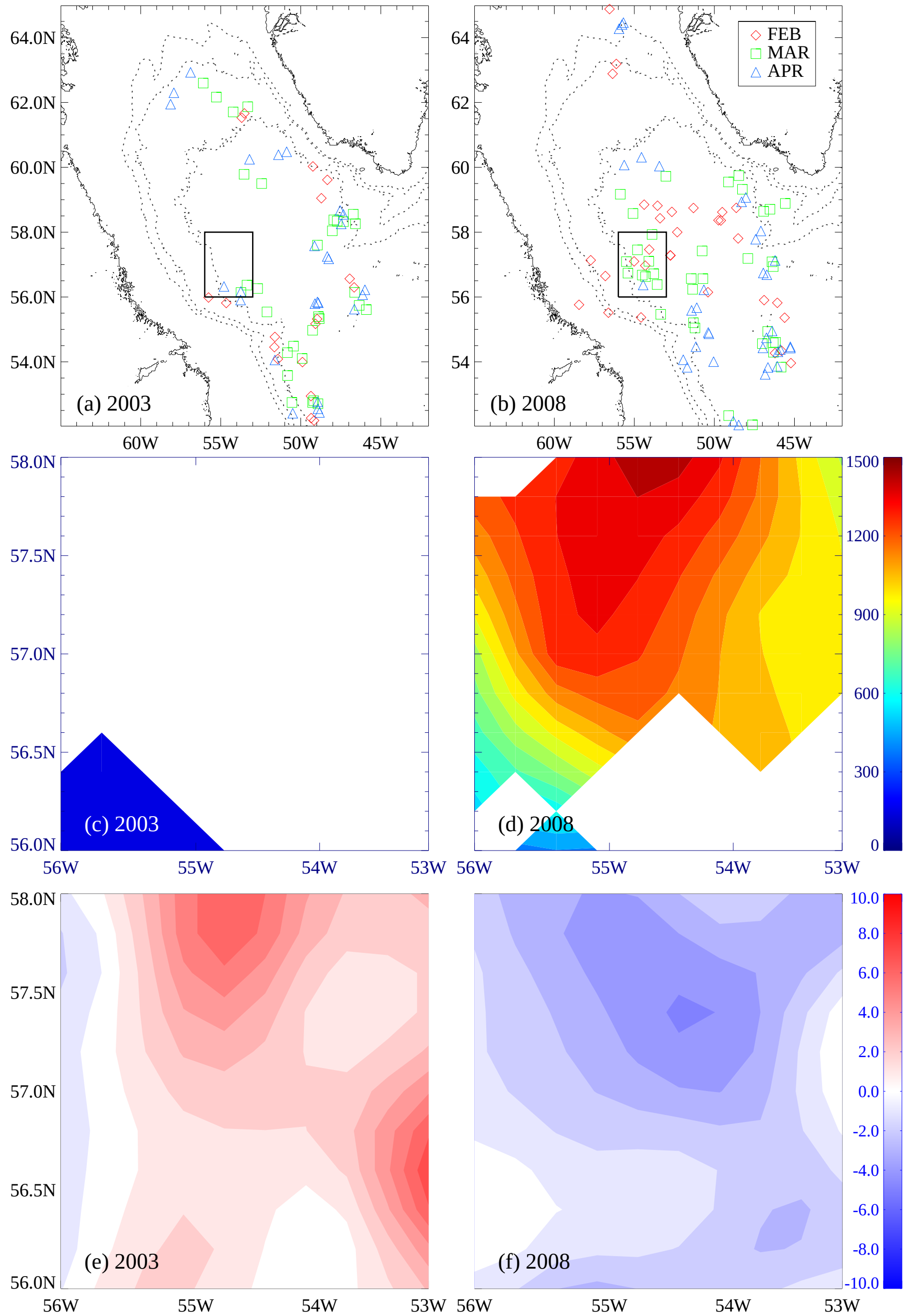

Figure 8. Locations of float profiles in the months of February, March and April in (a) a year with poor coverage in the central Labrador Sea (2003) and (b) a year with good coverage in the central Labrador Sea (2008). See Table 3 for the number of profiles on these and other years. The area in panels (c) to (f) is indicated in panel (a) and (b) by a rectangle. (c) Interpolated MLD map from the float profiles in February 2003 and (d) February 2008. (e) The SSH anomaly maps of February 2003 and (f) February 2008.

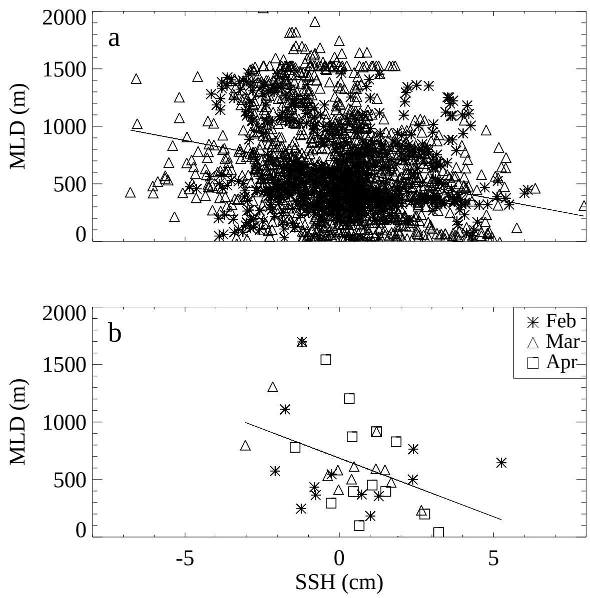

Figure 9. Relation between in the situ measured MLD and the SSH anomaly from altimetry data. (a) Scatterplot showing all valid data points between 56-58°N and 56-53°W (southwesternmost box in Figure 1 and rectangle indicated in Figure 8a and b) from the gridded MLD monthly maps. (b) As (a), but now the values are first averaged over 56-58°N and 56-53°W. This improves the overall correlation from -0.26 to -0.4.